Research Square

Preprints are preliminary reports that have not undergone peer review.
They should not be considered conclusive, used to inform clinical practice,
or referenced by the media as validated information.

Characterization, Indexing and Analysis of Motor Unit Activity During Muscular Effort by Multiple sEMG Integrated Signals

Yosafat Jetsemani Sámano-Flores
Instituto Politécnico Nacional (IPN)
Eduardo Morales-Sánchez
Instituto Politécnico Nacional (IPN)
Rogelio Campos-López
Universidad Politécnica de Guanajuato (UPG)
Julio Cesar Peña-Aguirre
Universidad Politécnica de Guanajuato (UPG)
Tomás Serrano-Ramírez
Universidad Politécnica de Guanajuato (UPG)
Antonio Hernández-Zavala
anhernandezz@ipn.mx

Instituto Politécnico Nacional (IPN)

Article

Keywords:

Posted Date: November 12th, 2026

DOI: https://doi.org/10.21203/rs.3.rs-11396276/v1

License: This work is licensed under a Creative Commons Attribution 4.0 International License.
Read Full License

Additional Declarations: No competing interests reported.

Characterization, Indexing and Analysis of Motor Unit Activity During Muscular Effort by Multiple sEMG Integrated Signals

Yosafat Jetsemani Sámano-Flores[1,2], Eduardo Morales-Sánchez[1], Rogelio Campos-López[2], Julio Cesar Peña-Aguirre[2], Tomás Serrano-Ramírez[2] and Antonio Hernández-Zavala[*1]

[1]Centro de Investigación en Ciencia Aplicada y Tecnología Avanzada (CICATA) – Instituto Politécnico Nacional (IPN), Querétaro, Querétaro, México.

[2] Universidad Politécnica de Guanajuato (UPG), Guanajuato, México.

*Correspondence: anhernandezz@ipn.mx

Abstract:

Background: Motor unit activity offers crucial information about muscle function and performance, providing invaluable data for diagnosis, treatment, and therapy. The parameters derived from this activity, such as the compound muscle action potential (CMAP) and motor unit number estimation (MUNE) extracted from the CMAP, are commonly obtained via electrical stimulation. While these methods provide specific insights into certain injuries and their impact on muscle function, their invasive nature presents a limitation. This work introduces an instrument capable of reconstructing and integrates multisignal sEMG (IEMG) as a high-fidelity indicator of CMAPs by convoluting MUAP (Motor Unit Action Potential) groups under controlled conditions, implementing an alternative noninvasive method with no electric stimulation to generate those sEMG-integrated multisignals (superficial IEMG) for our main objective, the characterization of muscle activity through the relationship between sEMG signals and force, an important indicator to complement CMAP. **Results:** The proposed system achieved a mean SNR of 14 ± 2.53 dB, a Pearson correlation of 0.907, and an nRMSE of 10.65%, results that robustly validate the precision of the IEMG model. This characterization accurately captures the electrophysiological dynamics of the quadriceps femoris during muscular effort, providing a continuous profile of muscle behavior. While this approach enables virtual MUNE estimation (averaging 85–147 motor units), **Conclusions:** Its primary significance lies in the methodology for characterize the muscle by integrated multisignals. This advancement provides a more accurate, streamlined tool for physiological assessment and physiotherapeutic diagnosis.

Keywords: CMAP, MUNE, IEMG, MU, Integrated multisignals, MUAP

Characterization, Indexing and Analysis of Motor Unit Activity During Muscular Effort by Multiple sEMG Integrated Signals

Abstract:

Background: Motor unit activity offers crucial information about muscle function and performance, providing invaluable data for diagnosis, treatment, and therapy. The parameters derived from this activity, such as the compound muscle action potential (CMAP) and motor unit number estimation (MUNE) extracted from the CMAP, are commonly obtained via electrical stimulation. While these methods provide specific insights into certain injuries and their impact on muscle function, their invasive nature presents a limitation. This work introduces an instrument capable of reconstructing and integrates multisignal sEMG (IEMG) as a high-fidelity indicator of CMAPs by convoluting MUAP (Motor Unit Action Potential) groups under controlled conditions, implementing an alternative noninvasive method with no electric stimulation to generate those sEMG-integrated multisignals (superficial IEMG) for our main objective, the characterization of muscle activity through the relationship between sEMG signals and force, an important indicator to complement CMAP. **Results:** The proposed system achieved a mean SNR of 14 ± 2.53 dB, a Pearson correlation of 0.907, and an nRMSE of 10.65%, results that robustly validate the precision of the IEMG model. This characterization accurately captures the electrophysiological dynamics of the quadriceps femoris during muscular effort, providing a continuous profile of muscle behavior. While this approach enables virtual MUNE estimation (averaging 85–147 motor units), **Conclusions:** Its primary significance lies in the methodology for characterize the muscle by integrated multisignals. This advancement provides a more accurate, streamlined tool for physiological assessment and physiotherapeutic diagnosis.

Keywords: CMAP, MUNE, IEMG, MU, Integrated multisignals, MUAP

1 Background

The integration of advanced technologies in physiotherapy has the potential to significantly improve patient outcomes and diagnostic accuracy by creating reliable environments and offering a wide variety of treatments as possible solutions. The use of innovative tools to study and characterize the function of muscles, such as surface electromyography (sEMG), plays a crucial role in enhancing our understanding of human performance and movement dynamics. These technologies provide valuable insights that can contribute to more precise diagnoses and personalized treatments.

The quadriceps femoris plays a crucial role in many kinematic human movements. Most human activities depend on proper walking mechanics. The quadriceps femoris and back are among the most common physiotherapeutic problems in Mexico. Injuries to the femoral quadriceps account for more than 30% of all cases reported in the country [30-31], which is a significant reason why people seek medical attention.

Parameters such as MU (motor units), CMAP and MUNE (Compound Muscle Action Potentials and Motor Unit Number Estimation) are important for muscle understanding. Several studies have used the CMAP as a key parameter for calculating the number of muscle motor units (MUs), which is critical since it provides information related to the number of MUs involved in the muscles in terms of voltage [42]. In [27], clustering was employed to identify and separate similar MUs on the basis of amplitude and duration from their specific technology. These data are used to calculate MUNE through averaging operations. In [29], electrical stimulators, CMAPs, and K-means clustering methods were combined to calculate the MUNE by summing the individual motor unit action potentials (SMUAPs) and averaging the results through arithmetic operations. MUNE techniques are clinically valuable for estimating the number of functioning motor units in a muscle. In [23], how to employ a protocol on the basis of the physiological space and position of the muscle was known. This protocol, in conjunction with the CMAP, is used to estimate the number of motor units. Additionally, knowledge was expanded in [17-18][28], with electrical stimulators to inject a constant current into the muscle, generating a CMAP, which was subsequently analyzed to relate the compound voltage to the average MUAP and calculate the MUNE.

Several methods calculate MUNE, such as numerical, arithmetic, and statistical tools, and their primary function is to understand muscle behavior under pathological conditions.

The methods for calculating MUNE are diverse, and a wide range of approaches are available, which expands the tools and applications within the field of physiotherapy [15]. Each method is based on a specific methodology, as in [16-18], [27], [29], [33] and [40] explain, which makes it valuable. However, this work identifies an opportunity to strengthen and further develop this area of science by addressing gaps that the referenced studies in this research do not focus on (IEMG) [47][48] and could be useful to reinforce the determination of muscle function.

The referenced studies included in this article address specific needs related to particular physiotherapeutic conditions [16-18], which limits the replication of their technology for different applications and reduces their scope in addressing broader problems. Moreover, most of these methods rely on the injection of an electrical signal as part of their technological function, as in [16-18], [27], [29], [33-34] and [40] mention, which decreases versatility and

flexibility. In contrast, the technology and results presented in this research are based on the analysis and processing of biosignals generated voluntarily and naturally by the body. This approach aims to provide a high-quality tool that can be applied more generally and under different physiotherapeutic conditions, making it more versatile and flexible. Importantly, the parameters computed in this work, such as the integrated sEMG (IEMG) and the virtual MUNE, are not intended to replace conventional CMAP and MUNE measurements. Instead, they represent indirect and complementary indicators that may contribute to a broader interpretation of neuromuscular activity within the limitations of nonstimulated signal acquisition.

The rest of this article is organized as follows. In Section II, we describe the background of sEMG signal generation, including context, antecedents, and their significance. Section III presents the construction and development of the instrument and methods, sensor acquisition, FPGA and MATLAB processing, and data visualization, also explain details of the experimental measurement procedure with the instrument, a metric protocol. Section IV introduces an integrated multisignal characterization of the sEMG force and a noninvasive technique to estimate the virtual (not real) number of MUs during quadriceps femoris movement. Section V provides a comparison and discussion of the technology and obtained results, and Section VI concludes the article.

1.1 sEMG biosignals and their electrical representations

The human body generates several electrical signals that provide insights into the functions of its biological components. Electric signals from the brain, heart and muscles, electroencephalogram (EEG), electrocardiogram (ECG) and electromyogram (EMG) respectively, are the primary types of electrical data used to obtain important information for health systems. Specifically, surface EMG (sEMG) provides detailed information about muscle activity. When a person thinks about moving a limb, an electrical pulse is generated in the brain and is transmitted through synapses to the spinal cord via a motoneuron. The motoneuron then connects to muscle fibers, allowing the pulse to propagate through the entire muscle. A single muscle movement does not generate just one motor unit action potential (MUAP); instead, hundreds of MUAPs are activated to produce a limb movement [17-18]. This information is crucial for developing better medical treatments that can improve people's quality of life, particularly in physiotherapy.

sEMG signals are challenging to capture because of their low amplitude and interference from biological noise caused by other physiological functions. This complexity makes it difficult for sensors and electronic devices to detect these signals during the initial stage of the acquisition of bioelectrical signals, specifically EMG.

Fig. 1 provides a general overview of the acquisition setups commonly used in sEMG research, which considers important parameters such as electrode distance, electrode position and electrode matrix shape, which are determinants of the quality of the signal. The outputs from these setups can be applied to various fields, including medical diagnostics, control systems, and signal processing [1-2] [6]. Fig. 1 illustrates typical acquisition circuits for electromyographic signals and serves as the foundation and context for further research into muscle force analysis and related applications [1-2][6].

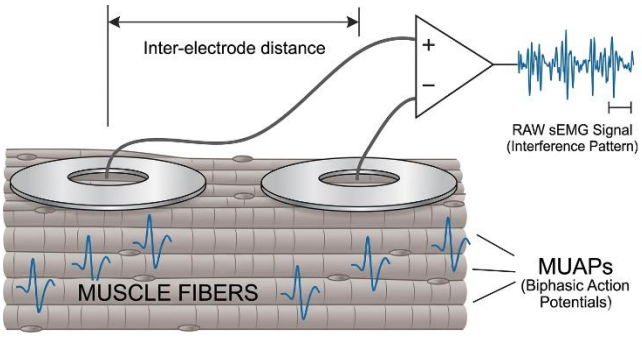


Fig. 1. The acquisition of pure sEMG signals is carried out via an operational amplifier with two electrodes in differential mode.

The methodologies and techniques for sEMG acquisition are primarily based on the use of multiple superficial electrodes. The differences between various studies lie in the electrode materials, shapes, matrix arrays, and muscles studied. However, they all share a common foundation of superficial acquisition via two or three derivation electrodes and a reference electrode for potential difference measurement.

sEMG trends reveal common factors in the setups and devices employed to achieve the objectives, which often focus on statistical applications, control, and pattern recognition. During the acquisition stage, systems prioritize the measurement of specific body parts, particularly where accurate data collection is most feasible [35]. In the conditioning stage, in addition to using instrumentation amplifiers with varying gains, most systems emphasize the development of filters for noise elimination [3], [4] and [5].

In the processing stage, there is a notable prevalence of microcontrollers as hardware and MATLAB as the preferred software platform. This setup provides a broad overview of the pathways and orientations in signal processing research, offering insights that can guide the development of new applications that stand out from those illustrated in Fig. 2. These applications, such as MUNE, are designed to calculate or provide critical information about muscular function. Determining the number of MUAPs offers valuable insights into correct muscular activity, such as CMAP

vs. force behavior and MUNE, in patients with neuromuscular disease [32] [33]. This type of research focuses on refining acquisition, processing, and numeric estimation methods to achieve these objectives.

Fig. 2 presents a diagram summarizing state-of-the-art advancements in sEMG research from recent years. The diagram highlights emerging trends in acquisition setups, hardware, processing power from PC processors, microcontrollers, digital signal processors (DSPs) and field programmable gate arrays (FPGAs). The feasible software for processing is mainly MATLAB and Python, and their diverse applications include statistics, signal processing and artificial intelligence (AI) systems.

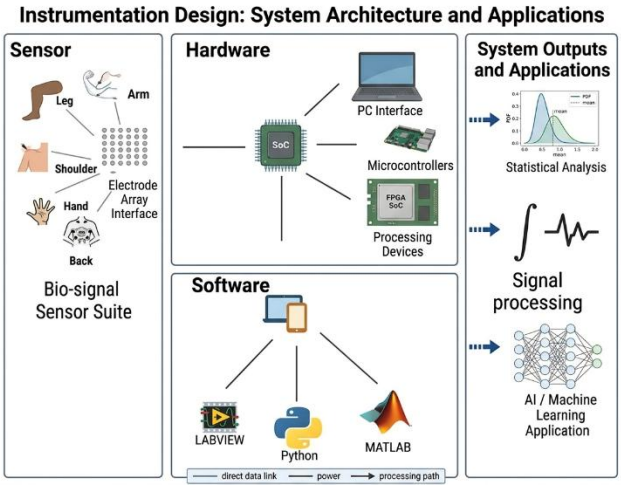


Fig. 2. The sEMG signals were acquired typically from five body parts: the biceps, legs, shoulder, and back. Hardware processed by embedded devices. Software processed typically by python and MATLAB. For specific applications.

The hardware used is FPGAs, DSP, and microcontrollers. The software used is LabVIEW, Python, or MATLAB. The main applications are in statistics, control, and artificial intelligence (AI). Within this context, the primary contribution of this work lies in the characterization and assessment of muscle activity through the physiological estimation of virtual MUAPs. This is achieved via a statistical and numerical method that relies on key input parameters, this number is not a real representation but show a clear relation between muscle activation and human movement. This approach is useful for the integration of expert systems, including the technology and method IEMG, CMAP and MUNE in other studies.

1.2 Electromyographic biosignals

sEMG is a technique used to measure the electrical activity generated by muscles during contraction and relaxation. Multiple voltage signals, known MUAPs, are generated by motor neurons in the spinal cord [9]. According to physiological references, an action potential with an approximate amplitude of 0.5 mV and a duration of 10–14 ms

originates in the corresponding MU and propagates through the muscle fibers as an electrical signal [24–25]. This signal is then captured by sensors and embedded devices for digital analysis [8] and [9].

The MU voltage is produced by a chemical process that creates a potential difference in the cells, propagating sequentially from the medulla to the muscle fibers. Multiple action potentials propagate through several muscle fibers simultaneously. These combined signals generate a raw sEMG signal. The integration of all these action potentials creates an IEMG signal parameter for the CMAP, as illustrated in Fig. 3. sEMG signals are acquired by an electrode on the body surface, and the voltage of the MU propagates in several muscle fibers. Fig 3. shows a RAW sEMG signal from the sensor, Voltage of several MUAPs, RAW motor unit action potential (MUAP), Amplitude of the MUAP and IEMG, index for CMAP indicator [19][20], serves as the foundation for the subsequent acquisition and processing steps.

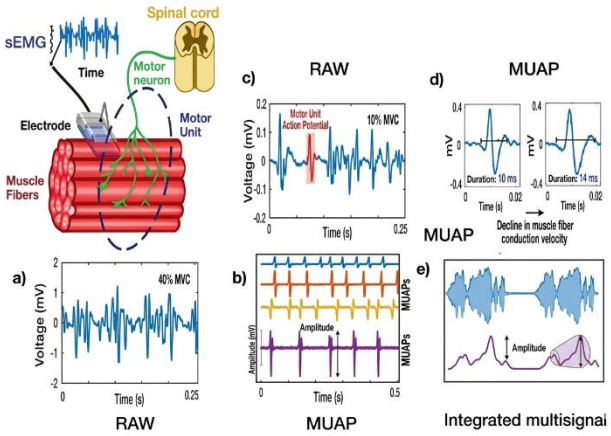


Fig. 3. The process of generating sEMG [19][20] is a) RAW sEMG, b) MUAP, c) multiple MUAPs, d) MUAP time and amplitude and e) IEMG.

1.3 Data acquisition architecture

The acquisition process is structured into distinct stages, as depicted in the diagram in Fig. 4. Initially, the signals are captured via an instrumentation amplifier in equation (1), which retains only positive values. In the final stage, the rectified signals are integrated, summed and convoluted over a specific time interval in an IEMG with equation (3) and further amplified with equation (4) to prepare them for processing in FPGA and MATLAB with several methods, such as digital conversion, multiplexing, filtering and numeric equations. Then, the information from electrical and physiological analysis is displayed by the algorithms from IEMG and effort relation and estimation.

In first stage with equation (1), multichannel sEMG acquisition provides detailed information about muscle behavior. Two D array electrodes positioned on the muscle surface can vary in number and geometric arrangement.

Extending this concept, other arrays are based on 2D arrays but incorporate a third parameter, such as volume or impedance. Two-dimensional arrays are further divided into two categories: high-density sEMG (HD-sEMG) and high-spatial-resolution sEMG (HSR-sEMG). Each category has distinct characteristics and technical specifications. The second refers to identifying a small zone in the muscle and performing a thorough analysis, especially for estimated motor unit action potential recruitment. System here is scalable and supports arrays mentioned before. To generate integrated multibiosignals (IEMGs), the system employs an operational amplifier in an integrated configuration combined with a digitizer embedded within the device. The raw signals are captured via an operational amplifier (op-am) and subsequently conditioned through several stages. The stages of this process are mathematically represented in equations (1), (2), (3), and (4).

$$V_{RAW} = A(Va - Vb) \tag{1}$$

$$Vs(t) = \frac{d}{dt}[V_{RAW}] \tag{2}$$

where $Va - Vb$ is the differential voltage between muscle cells, A is the Op–Am gain, V_{RAW} is the sEMG signal in the Raw state and Vs is the output voltage.

$$Vi(t) = -\frac{1}{RC}\int Vs(t) - \frac{Rf}{R}\, Vo(t)dt \tag{3}$$

where Vo is the voltage under ideal conditions, Rf is the feedback resistor, R is the design resistor, and C is the capacitance and Vi is the output voltage from five block.

$$Vout = -Vi\left[\frac{R1}{R2}\right] \tag{4}$$

where $\frac{R1}{R2}$ is the amplificatory gain in the final stage and where $Vout$ is the integrated voltage used for processing.

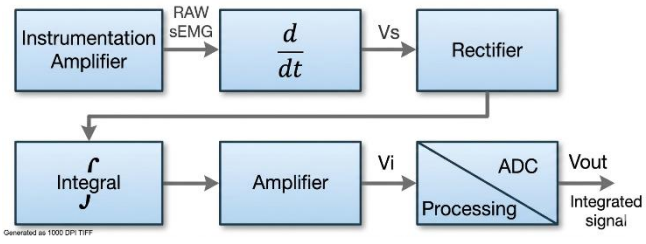


Fig. 4. The different stages of the acquisition system include filtering, rectification, integration amplification, conversion and processing of the sEMG signal.

1.4 Motor unit estimation fundamentals

The main characteristics of a motor unit include its amplitude, spatial distribution, and time parameters. These factors are essential for estimating MU numbers [19] and [20]. When combined with technical specifications such as

198 frequency, gain, noise elimination, electrode type, electrode placement, material properties, and integrated signal
199 analysis, these factors provide tools for MUNE. Estimating motor unit numbers is critical for diagnosing and
200 monitoring various neuromuscular diseases. Recent advancements in electromyographic techniques have
201 significantly improved the accuracy of these estimates. Research has evaluated the reliability of motor unit
202 estimation via CMAP analysis across different muscles and research centers [16].
203 For example, MScanFit is an important tool that has been used to estimate motor unit numbers and monitor muscle
204 recovery in individuals with diabetic polyneuropathy [17]. It has also been applied in patients with myotonic
205 dystrophies, and its effectiveness has been tested in these specific conditions [18]. Additionally, studies have
206 introduced the motor unit number index (MUNIX) [23], exploring its principles and applications for both healthy
207 individuals and those with motor neuron disease. Also, the use of high-density surface electromyography (HD-
208 sEMG) for motor unit number estimation has been investigated and has improved accuracy [27].
209 Research on the topography of motor unit action potentials has also contributed to more precise motor unit number
210 estimation [28]. Finally, recent advancements in high-density surface electromyography decomposition have further
211 refined motor unit number estimation, enhancing the overall analysis [29]. These studies underscore the progress
212 made in technology and methodology for assessing motor unit numbers, providing valuable tools for both clinical
213 and research purposes.

214 ## 2 Results

215 This section is divided into three subsections: the first covers multisignal processing and analog-to-digital
216 conversion; the second shows the relationship between muscle force and MUAP activation; and the third introduces
217 IEMG, a new noninvasive method as index for CMAP and MUNE.

218 ### 2.1 Results of multibiosignals processing

219 The module includes a four-channel surface electromyograph; each channel has two leads (red, green) and a shared
220 reference electrode (yellow). This setup is connected to another module for signal conditioning and processing. The
221 raw data are displayed on an oscilloscope, while the digitally integrated data [16][22] are shown in MATLAB, as
222 illustrated in Fig. 5. The acquired sEMG signals are displayed on a computer with MATLAB software, marking the
223 first digital visualization process. The digitally IEMG signal generated by the proposed system is presented. The
224 acquisition stage and the FPGA for the sEMG processing unit are illustrated in Fig. 5, where the system is
225 interconnected.

Furthermore, the sEMG processor is connected by an interface with a computer for data analysis in MATLAB, where the graphical results are obtained, including the digitally IEMG signal and its relationship with muscle force. The experimental setup also includes a muscle connection and electrode placement on the human knee. This aspect is particularly important, as electrode positioning and interelectrode distance significantly affect the accuracy of IEMG measurements for signal indexing helping for the estimation of motor unit number, is a general system for fundamentals an specific injuries studies.

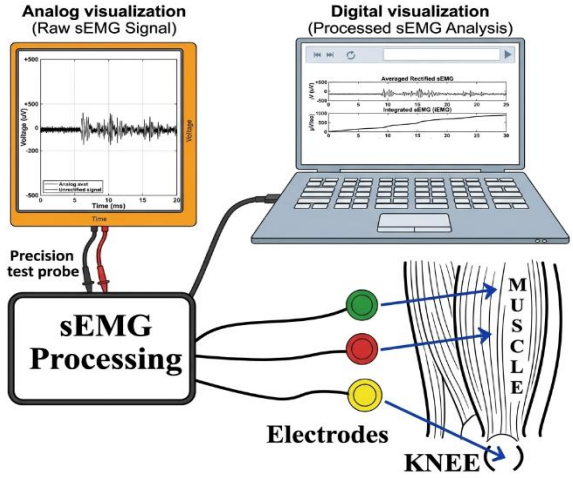


Fig. 5. The measurement module is composed of an electrode connected to the femoral muscle. Analog signals are shown in the oscilloscope. The digital integrated sEMG signals are shown on the computer.

Each of the sEMG signals of the four channels are conditioned, captured and summed through the integrator configuration to generate an IEMG signal via an integrator and then digital processing, as illustrated in Fig. 6 and described in equation (5).

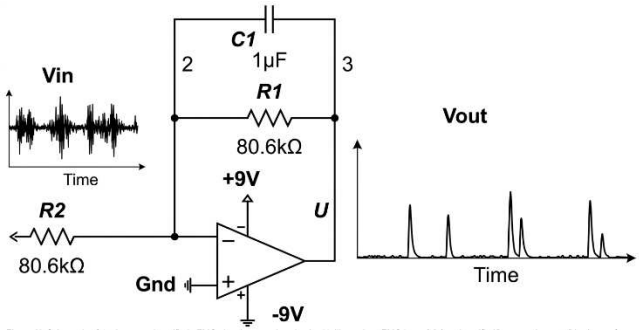


Fig. 6. An integrated amplifier adds the voltage amplitude of every MUAP at a specific instant and provides an integrated signal of the lineal muscle response. The capacitor determines the CMAP time.

Each of the four sEMG biosignals captures variations in the electrical potential produced by muscle cells when activated, each one in a particularly position of muscle.

At this stage, the circuit performs a mathematical operation by calculating the integral of the signals with respect to time over a defined interval. This process is typically implemented via an operational amplifier configured for integration, as expressed in equation (5) and (6). Considering ideal conditions, we can eliminate noise and offset it via acquisition sensor characteristics:

$$Vout_{CMAP}(t) = -\frac{1}{RC}\int Vin_{sEMG}(t)\,dt \tag{5}$$

$$Vout_{CMAP}(t) = \frac{1}{(80.6K\Omega)(1uF)}\int Vin_{sEMG}(t)\,dt \tag{6}$$

where Vin_{sEMG} is the voltage measured in the muscle, RC is the integration factor and $Vout_{CMAP}$ is the output integrated voltage.

The circuit's output produces a continuous digital signal that increases over time as muscular effort intensifies and decreases as the muscle enters a relaxation state, as illustrated in Fig. 7. The integrator accumulates and smooths MUAPs to generate IEMG biosignals. A clear relationship is observed between the increase in effort and the corresponding increase in the amplitude of the IEMG voltage signal, where each peak corresponds to a specific muscle effort [10-14][42].

Fig. 7 shows the transition between analog biosignal raw sEMG and digital biosignal IEMG and MUAP segmentation.

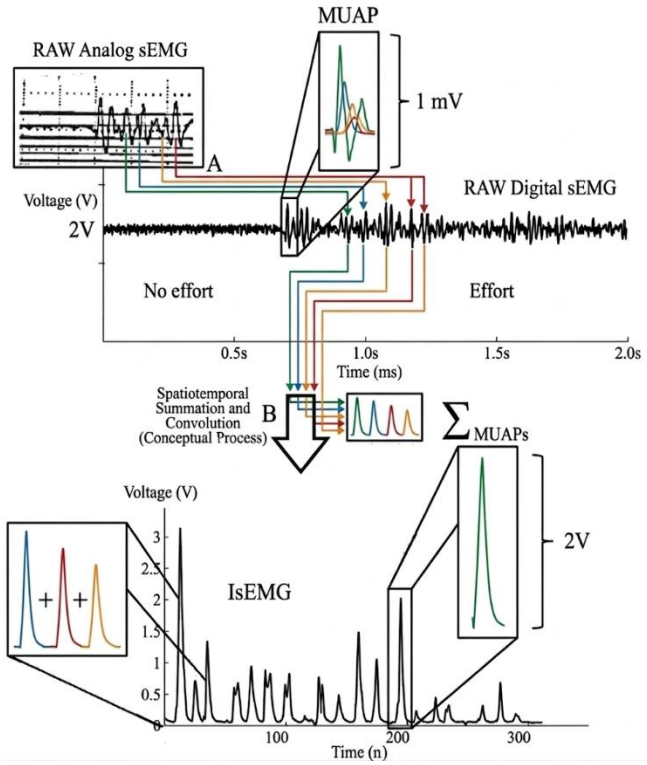


Fig. 7. The integrated signal sample A) shows a RAW sEMG signal, where every peak represents one singular motor unit action potential

(MUAP), and B) shows the compound muscle action potential, which represents the sum of the MUAPs in a time interval.

The flexion-extension movement in the leg provides a IEMG signal with a voltage amplitude response by the movement routine. This routine is digitally represented in this specific case by vectors of 1000 samples in 90 seconds define for experiment, as shown in Fig. 8. These signals are processed and presented as four separate graphs, which represent the integrated sEMG signals and their respective IEMG signals [16][22] from one user movement in respective muscle function.

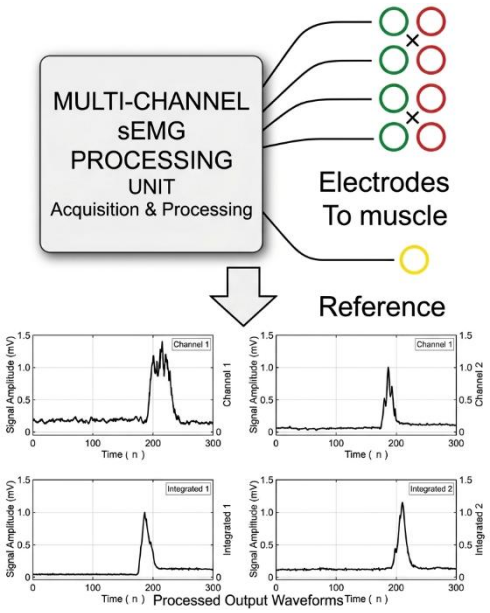


Fig. 8. The four-channel sEMG signals were acquired. Multiple signals are processed. The four sEMG integrated and digital signals are shown.

The four channels system, with the possibility to expand to additional channels if needed. These four channels provide the experiment with integrated multisignal sEMG, consisting of four IEMGs recorded from different positions in the rectus femoris. The four multisignals are multiplexed via a time-division algorithm implemented on the FPGA and are displayed in a single graph, which represents a unique event for each user. The channel function visualizations are individually shown in Fig. 9. Asynchronous testing on four channel to ensure functionality.

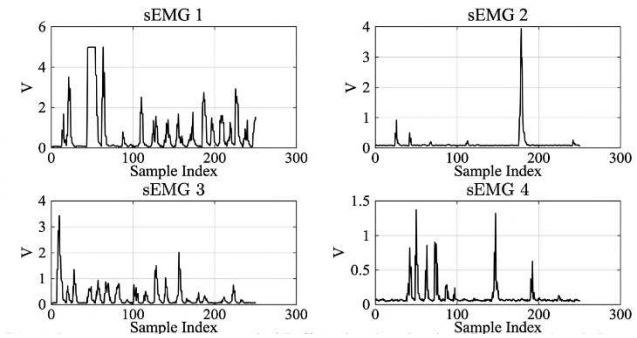


Fig. 9. Graphics for each of the four channels shows the electric response of the flexion extension of the leg.

Now in Fig. 10, the user performs a specific exercise, moving the rectus femoris muscle from the sitting position one with the feet on the ground to position two with the leg extended and flexing the right leg from 90 degrees to 180 degrees, as further detailed in the subsequent figures. The four integrated multisignal IEMGs represent the user's muscular effort during movement, the extension effort corresponds to an increase in the signal's voltage amplitude, whereas the relaxation during flexion is associated with a decrease in the voltage amplitude. During the official experiment, the four integrated multisignals were synchronized for simultaneous recording and analysis, as shown in Fig. 10 and 11.

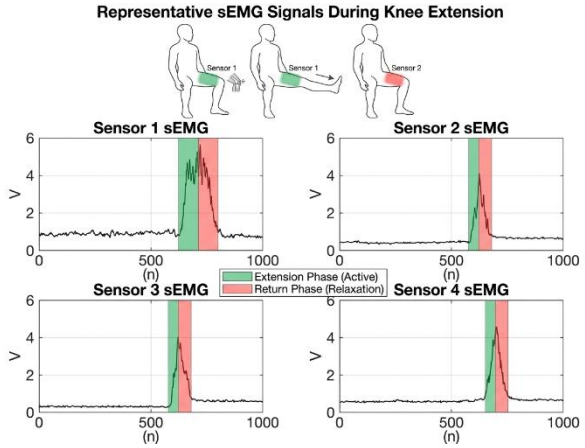


Fig. 10. The flexion–extension movement in the leg is represented by the sEMG integrated signal as a voltage amplitude response. The movement routine was performed on 1000 samples in 90 seconds.

A sensor with a four-channel arranged matrix is placed on different regions of the rectus femoris muscle. It acquires four IEMG signals. It functions at a specific location. These signals are displayed as four separate graphs, as shown in Fig. 11. They illustrate the effort involved in the flexion–extension of the left leg, with the only variable being the electrode position.

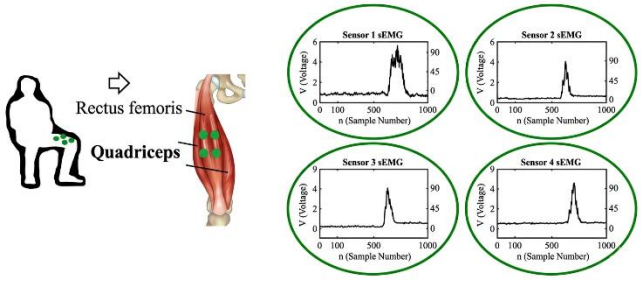


Fig. 11. The image shows the graphics of four channels in the flexion–extension routine movement. These four signals represent the electric response of the femoral muscle in four different positions in the same movement route.

2.2 Results of the IEMG characterization

The sEMG muscle behavior illustrated can be compared to the force behavior shown in equation (8), as depicted in Fig. 12. In the image, we can see how the sEMG increases with the help of integration behavior from the integrator arrangement [21]. The IEMG voltage increases as individual motor unit action potentials (MUAPs) are recruited, summed, and convoluted in both amplitude and time, a process that generates the integrated voltage referred to as IEMG. This relationship is governed by a sequential process where muscle movement triggers the activation of a specific number of MUAPs. Under controlled initial conditions, this number remains approximately constant until they are captured by the integrator circuit, which constructs the integrated biosignal. Consequently, as a greater number of MUAPs processed and summed, the resulting IEMG voltage increases proportionally shown in Fig. 12, validating the direct dependence between motor unit recruitment and the synthesized signal.

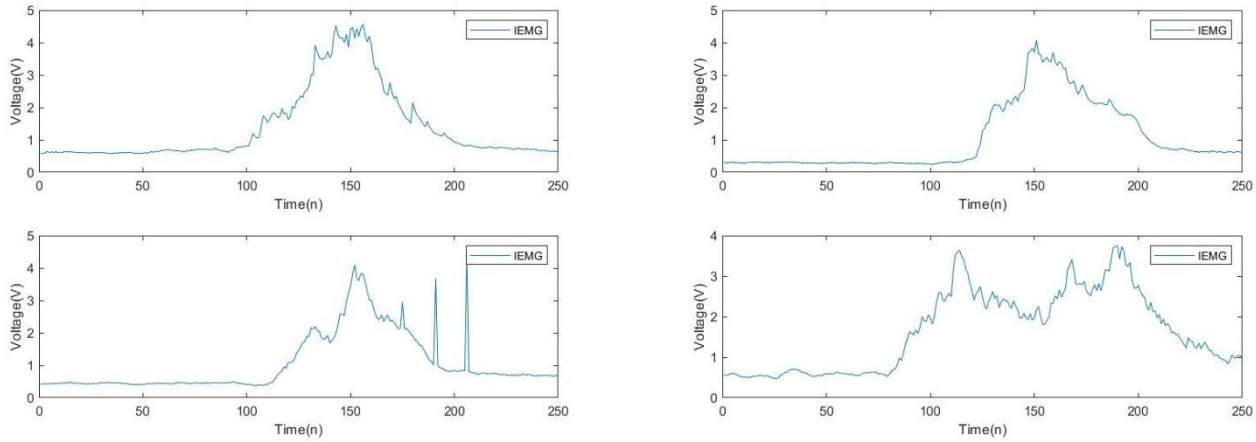


Fig. 12. The voltage sEMG increases as the charge integrator response increases. The sEMG voltage increases with discrete time on the horizontal axis.

There is a relationship between the sEMG voltage and the force voltage, as shown in equation (7) and equation (8).

$$V_{sEMG} = Vin * e^{\frac{-1}{t}} \quad , \quad t = RC = 0.0806 \tag{7}$$

$$V_{Force}(t) = \frac{R1}{R1 + R2} * Vin_{Force}(t) \tag{8}$$

where V_{sEMG} is the voltage from the muscle, t is the time, and V_{Force} is the output voltage from the force sensor.

The signal acquisition stage demonstrated high reliability across all experimental trials. The calculated Signal-to-Noise Ratio (SNR) values for the four primary datasets were an average SNR of 14 ± 2.53 Db [44][45]. These results confirm that the instrumentation stage, centered on the instrumentation amplifier, successfully isolated the physiological sEMG signals from environmental interference, providing a robust foundation for the subsequent force

characterization model.

In experiment the user applies force to the sensor, both the force sensor and the muscle are activated, resulting in an increase in their respective signals, as shown in Fig. 13. A strong linear relationship was observed between the IEMG signal response and the activation of MUAPs during muscle movement. This relationship is illustrated in Fig. 13, where the correlation coefficient (r = 0.90764) and the significance level ($p < 0.01$) indicate a highly significant correlation. Additionally, the coefficient of determination ($R^2 = 0.824$) demonstrates that the model accounts for 82.4% of the variance, confirming a robust predictive strength and a clear dependence between the measured variables.

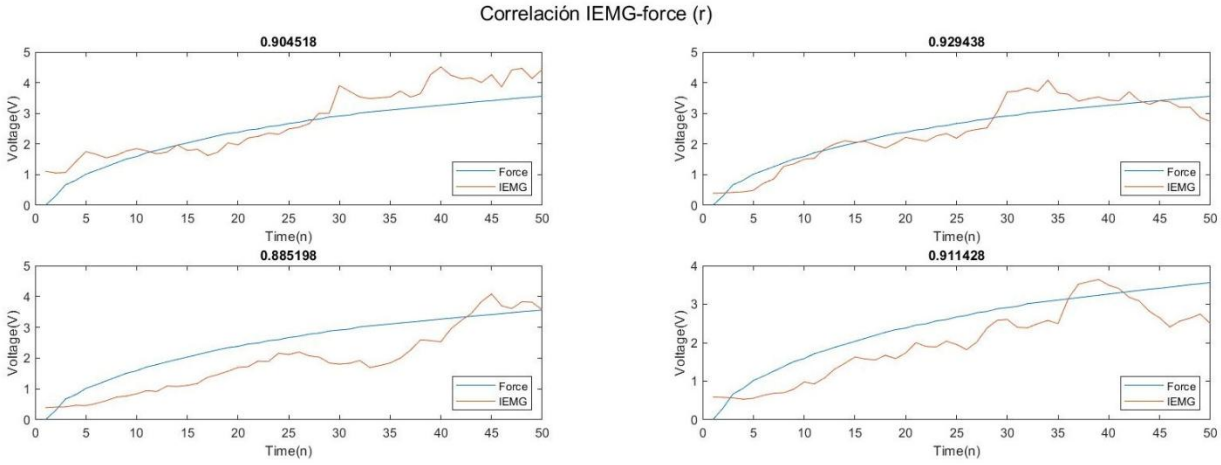


Fig. 13. Force/IEMG relation, in the four graphics from four sensors are shown the increase relation between IEMG and force.

Furthermore, the Root Mean Square Error (RMSE) was employed to validate the predictive model. In this study, the model estimates the relationship between the IEMG signal and muscle force, as denoted in Equation (9). The corresponding results are summarized in Table 1.

$$RMSE = \sqrt{\sum_{i=1}^{n} \frac{(y_i - \hat{y}_i)^2}{n}} \quad (9)$$

Where y is a present sample, $\hat{y}_i$ is average sample and n is the length of sample vector.

Table 1

nRMSE from results experiment measurements

Sample	1	2	3	4
nRMSE	10.89%	9.42%	11.88%	10.51%

The normalized RMSE (nRMSE) expresses the error on a 0–100% scale. Values between 10% and 20% indicate an accurate correlation, accounting for the inherent variability of a dynamic experiment. These results reinforce and validate the proposed model.

2.3 Results of MUAP indexing

As proposed in this work, the data obtained can be used to estimate the instantaneous number of MUAPs through equation (7), which represents the sEMG voltage behavior, and equation (8), which represents the force voltage behavior. Under optimal conditions, the muscle will maintain an increased voltage in both signals, the sEMG and force when the muscle's sEMG increases from its minimum voltage to its maximum voltage, as shown in Fig. 14. By analyzing the system gain and MUAP, as shown in Tables 3 and 4, virtual MUNE can be estimated. A virtual number can show an excelent idea from muscle behavior not a exact quantity. [16-20].

To ensure experimental accuracy, several critical conditions must be strictly controlled, including the time to fatigue and capacitor charging intervals, the system offset, and the initial supply voltages. Furthermore, maintaining a constant sEMG gain and standardizing electrode dimensions, materials, and positioning is essential to guarantee the reproducibility and validity of the recorded physiological data. Strict control over these parameters is vital, as minor variations can compromise the accuracy of all subsequent calculations. By maintaining these factors, the experiment ensures reliable results for the proposed virtual MUNE calculation method during femoris flexion–extension, utilizing the optimized IEMG-to-force relationship defined in equation (10)

$$V_{CMAP}(t) = \sum_{t=0}^{T} Vin_{sEMG}(t)\Delta t \tag{10}$$

where Vin_{sEMG} is the input muscle voltage, V_{CMAP} is the output integrated voltage from the instrument and t is time.

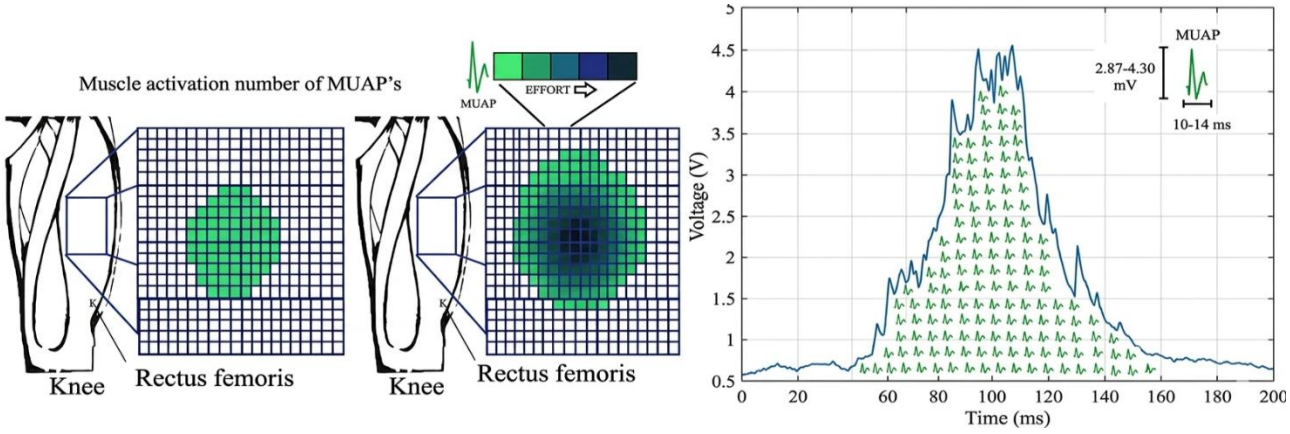


Fig. 14. The voltage amplitude of the MUAPs is approximately 1 mV, with a 10 ms duration in the minimum range and 14 ms in the maximum range. Mathematically, the recruitment from 10 ms is approximately 5.7 MUAPs, and the recruitment at 14 ms is 8 MUAPs. The system gain is 11 times the sEMG voltage generated by the muscle, meaning that the final CMAP is divided by that gain to obtain the final number of MUAPs.

2.4 IEMG biosignal analysis and virtual MUNE

IEMG signals from seven participants were measured and recorded in Tables 2 and 3. The IEMG, which includes specific data from every participant, was used to calculate the virtual MUNE. Virtual MUNE (vMUNE) was obtained via numeric calculation. for every participant with their corresponding IEMG, gain and MUAP recruitment in the maximum and minimum ranges. We can observe the MUAP calculation from 10 ms of system gain, IEMG and vMUNE from seven participants in Table 2. Table 3 shows the MUAP calculation from 14 ms of the system gain, IEMG and vMUNE from seven participants. In both cases, the gain from the system is 11.

Table 2.

Motor unit number estimation from the 10 ms MUAP duration

Sample	1	2	3	4	5	6	7
MUAP (mV)	0.00403	0.00403	0.00403	0.00403	0.00403	0.00403	0.00403
IEMG (V)	4.428710	4.667968	3.75	4.394531	4.077148	4.560546	4.677734
vMUNE	99.9032	105.3004	84.59282	99.13221	91.97266	102.8772	105.5207

Table 3.

Motor unit number estimation from the 14 ms MUAP duration

Sample	1	2	3	4	5	6	7
MUAP (mV)	0.00287	0.00287	0.00287	0.00287	0.00287	0.00287	0.00287
IEMG (V)	4.428710	4.667968	3.75	4.394531	4.077148	4.560546	4.677734
vMUNE	140.282	147.8609	118.7836	139.1995	129.1462	144.4582	148.1702

The virtual numbers estimated for every user for the MUNE results are shown in Fig. 15. We can observe the values from every participant in the range from the minimum to the maximum vMUNE. For the graphical results, the minimum 10 ms and maximum 14 ms MUAP durations were used.

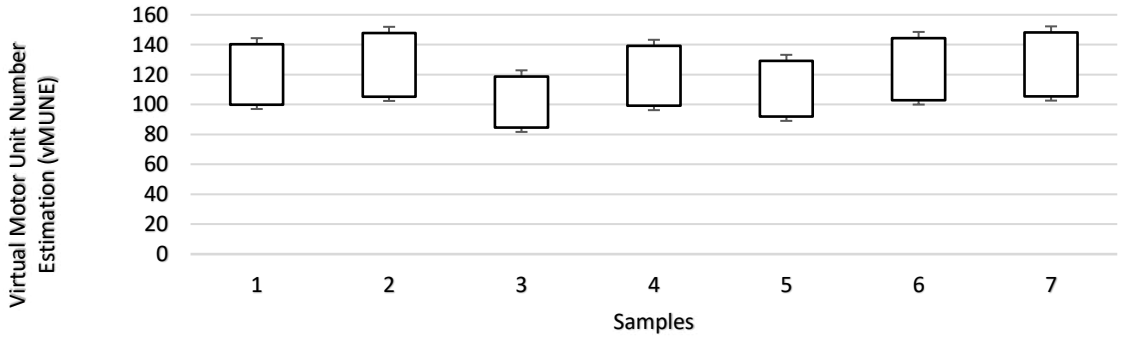


Fig. 15. Motor unit number estimation for seven participants, with specifications from theoretical sEMG information and system design.

3 Comparison and Discussion

Table 4 presents the virtual MUNE values reported by several authors cited in this article, with the aim of correlating their results with the methodology proposed here. A certain convergence among the values can be

observed; however, it is important to emphasize that each method differs from the others in terms of signal acquisition and conditioning, the processing techniques employed, and the visualization approach. Notably, differences result from electrode positioning and the specific muscle monitored. Therefore, the significance of each contribution lies primarily in the application of the method, the technique, and the measurement instrument.

Table 4.

Comparison of studies.

Method	Invasive	Stimulation	vMUNE	Approach	Method
Sorensen [16]	No	Yes	150	0.980	MScanFit CMAP scan, noninvasive, incremental stimulation
Kristensen [17]	No	Yes	110	0.748	MScanFit, using electrical stimulation for MUNE
Schneider [18]	No	Yes	73-109	0.741	MScanFit in dystrophies, electrical stimulation
Van Dijk [27]	No	Yes	271-290	0.014	MUNE by HD-sEMG, electrical stimulation used
Peng Y [29]	No	Yes	191	0.701	MUNE by HD-sEMG, electrical stimulation used
Arnold [33]	Yes	Yes	278	0.112	Invasive technique with electrodes
Chen [34]	No	No	118.1	0.797	MUNE without stimulation or M-wave recording (noninvasive)
Goker [40]	No	Yes	300	0.041	Study with simulations, CMAPmax-MUNE relationship, stimulation used
In this work	No	No	85-147	1.00	sEMG Integrated Multisignals (CMAP), noninvasive.

This study proposes an approach for the characterization of muscle behavior through the integrated multisignal (IEMG) of multichannel surface electromyography (sEMG) signals, force measurements, and virtual motor unit number estimation (vMUNE) by utilizing an array of electrodes. Compared with conventional systems, this method captures a more extensive set of electrical, dimensional, and geometric information, as explained in [1-3], [5] and [35], and provides a review of the main surface electromyography (sEMG) configurations and some of their key characteristics, forming the foundation for a research database and providing a detailed analysis of muscle activity. The study highlights a direct relationship between the increase in sEMG signal amplitude and the force applied by the user, similar to those from [16], [18], [22] and [36], where invasive methods are used to generate CMAPs and are used mainly to address specific disorders. This is achieved by evaluating the sEMG activity of the femoral muscle and the corresponding force data. Furthermore, some authors, such as [16], [18], [37], and [38], introduced methods for estimating the number of motor units (MUs) involved in muscle contraction with the integration of signal IEMG and force voltage data. This enables the estimation of the number of virtual MUs, such as those based

391 on action potential characteristics. They identify a relationship in the increasing number of MUs with the increasing
392 effort of the users. This work with non-invasive techniques reinforces the MU count of invasive methods when
393 injecting an electrical stimulus presented in [17] and [18] with similar virtual MUs (90-180), but it differs in that
394 number of MUs in [38] (<20). This is because of the characteristics of the electromyograph configuration, such as
395 gain, offset, interference, number of electrodes and numeric calculations, along with the physiological parameters,
396 such as the specific muscle, its dimensions, the area considered and the user.
397 It is possible to use techniques to determine a virtual number of motor units during a muscle activation process. The
398 available technology allows for the decomposition of sEMG signals and multichannel arrays, increasing the amount
399 of information obtained from the muscle. Current studies provide solid support for these results. Each technique,
400 such as the one proposed in this work and those referenced here, contributes to and reinforces the accuracy of the
401 calculations. However, as mentioned earlier, this also involves significant challenges that depend on the specific
402 conditions of the study and the experimental setup [15]. Although vMUAP quantification is an estimation under
403 controlled circumstances, some studies use a disorder parameter to characterize MUNE.
404 With specific guidelines, it offers valuable insights into muscle function and fatigue, which can be particularly
405 useful in physiotherapeutic assessments. The scope of the IEMG and vMUNE methods in here, as well as their
406 objectives, can vary greatly depending on the application. Therefore, this research provides a clear foundational
407 context and a very specific objective. The scientific contribution of this research lies in refining the vMUNE
408 quantification technique, the force-sEMG characterization and the IEMG-effort relation by incorporating numerical
409 methods for improving accuracy and a low-cost acquisition instrument. The proposed method provides more reliable
410 estimates of virtual MUs and enhances the precision of motor unit analysis by optimizing key experimental
411 parameters such as time to fatigue, sEMG gain, and electrode positioning. The physiological specifications, such as
412 MUAP amplitude and duration, are defined in [19-20], and the instrument for IEMG measurement depends on its
413 technical construction, such as acquisition, rectification, noise reduction, gain and density of the electrode array, as
414 defined by the designer.
415 In summary. The scientific contribution of this research lies in enhancing the accuracy of motor unit estimation by
416 the following:
417 -Refining vMUNE quantification through improved numerical methods.
418 -Strengthening the relationship between the IEMG, MUAP activation and muscular effort.

-Optimizing experimental parameters such as the time to fatigue, noninvasive electrode placement, and acquisition settings.

- Low-cost sensor and instrument acquisition design and construction.

This approach has the potential to advance diagnostic and monitoring tools for neuromuscular diseases, offering a more accurate and detailed understanding of motor unit behavior during muscle contraction. These technologies also contribute to optimizing the diagnostic process, offering different methods to obtain more information for better biosignal analysis. The contribution of this approach is that it expands the technological options available for medical treatments and offers a novel way to generate a femoris characterization and extract quantitative virtual data (vMUNE) from muscle activity, which is essential for muscle monitoring, treatment and diagnosis. The ability to prevent quadriceps femoris-related problems through early detection and monitoring is crucial for maintaining an active and healthy lifestyle. Technologies that offer detailed information about muscle function can complement the expertise of medical professionals, enabling more accurate evaluations and custom interventions.

4 Conclusion

This work confirms the existence of a correlation between the muscular effort and the generated voltage by reconstructing integrated signals (IEMGs). These are obtained through noninvasive methods, providing valuable information from muscle function, such as the virtual motor unit number estimation (vMUNE). By focusing on muscle characterization and the estimation of virtual motor units (MUs), the results also correlate with the results of other authors, even though there are differences in acquisition, conditioning, processing, visualization, electrode positioning and muscle monitoring. This study demonstrates how integrating technology into the physiotherapy process can improve therapy information parameters to improve medical practices. The world needs more accessible technologies for health care treatment to improve quality of life and save more lives.

5 Methods

The components shown in Fig. 16 illustrate the system's architecture, integrating sensors, processing, and visualization blocks. Signal acquisition is performed by the instrumentation amplifier, selected for its high CMRR (83–96 dB) [43] and low-power characteristics ideal for biopotentials. The processing block utilizes FPGAs for biosignal multiplexing and high-speed processing to reconstruct the four sEMG integrated signals (IEMG). A central objective is analyzing the IEMG–Force correlation during rectus femoris flexion–extension routines, providing a continuous profile of muscle effort. MATLAB algorithms then apply numerical and statistical tools to calculate a

virtual MUNE (vMUNE) via this non-invasive approach. Furthermore, the software environment manages data visualization, plotting the integrated signals alongside the estimated number of activated MUs and their corresponding statistical results. This integrated framework ensures that raw physiological data is transformed into actionable diagnostic metrics through robust mathematical validation. By synchronizing high-fidelity hardware acquisition with advanced computational analysis, the system achieves a reliable characterization of motor unit recruitment patterns.

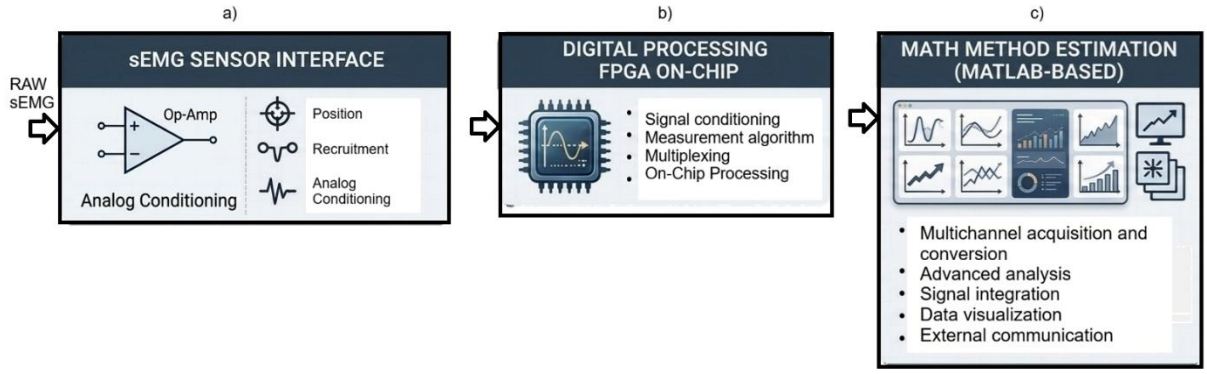


Fig. 16. a) Acquisition stage, b) signal analysis and c) signal display

This investigation has led to the development of a system for the acquisition and processing of dimensional, spatial, and electrical data, with a focus on the relationship between the rectus femoris force and the integrated IEMG digital signal. The proposed system estimates motor units on the basis of basic parameters of the action potential, such as the amplitude and duration of MUAPs, which contribute to the amplitude of the IEMGs [19] and [20]. The integrated sEMG signal [16][22] provides an approximation of the motor neurons involved in generating the electromyographic signal of the rectus femoris. This phenomenon is directly correlated with muscle function [40], [41], particularly its crucial role in supporting most of the human body's weight during various activities.

Fig. 17 shows the acquisition results obtained via acquisition sensor, which are then conditioned and integrated with an operational amplifier array. The integrated analog voltage is then converted to a digital voltage via a 10-bit resolution analog-to-digital converter (ADC), which is multiplexed and processed in FPGA, and the numeric calculus, analysis and visualization are computed in MATLAB [7].

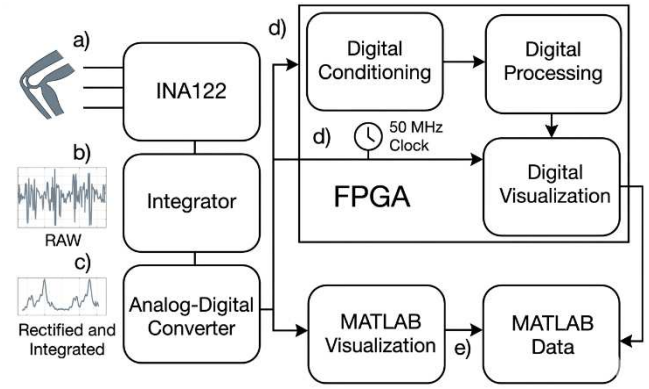


Fig. 17. Block diagram of the complete process from characterization and MUAP estimation: a) Instrumentation operation, b) Integrator operation, c) digital conversion, d) FPGA processing and e) MATLAB processing.

5.1 Acquisition instrument design

The Acquisition involves integrating the signal through the integrator operational amplifier shown in Fig. 18, which generates the integrated signal (IEMG).

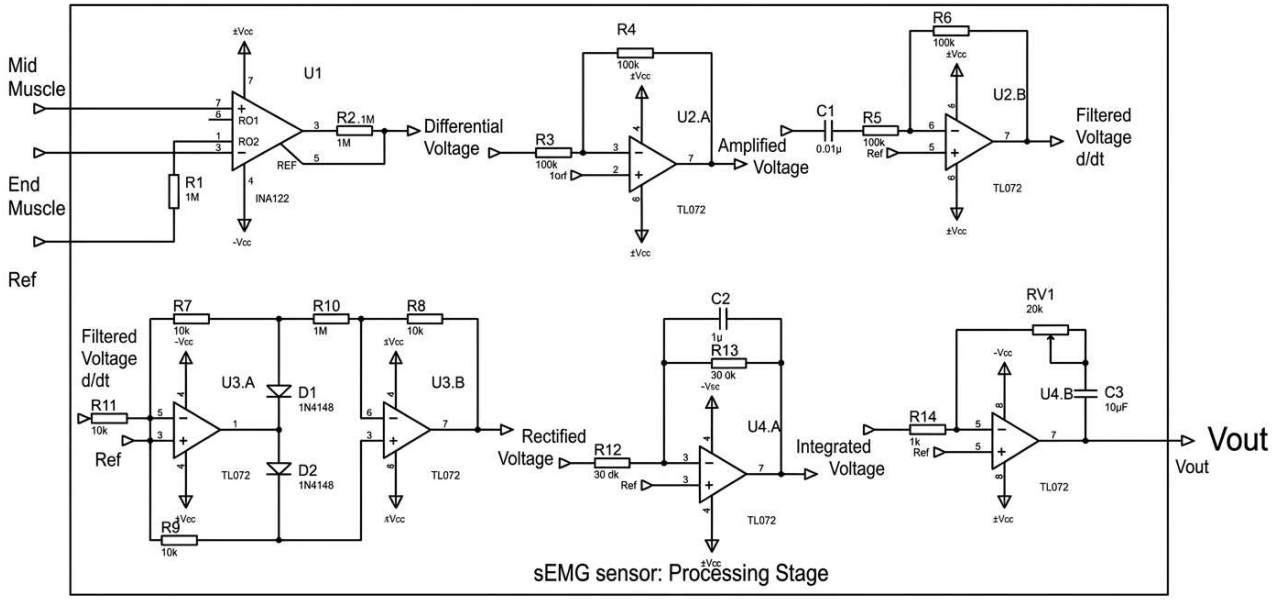


Fig. 18. The muscle voltage is acquired by the operational amplifier INA122 and then amplified in the following stage. In the next stage, the voltage output is rectified and then integrated by an operational amplifier integrator. In the final stage, the voltage is amplified by a variable POT.

First the circuit is primarily implemented via operational amplifiers connected in sequence, with each device serving a specific conditioning function. The process starts with the instrumentation amplifier, ensuring robust signal acquisition with a CMRR of 83–96 dB [43] to effectively minimize common-mode

noise in the sEMG recordings. The signal is then filtered through a differential configuration to eliminate noise. The next stage rectifies the voltage amplitude, allowing only positive components to pass. This process sums the voltages from each muscle fiber during movement; this electronic device is a low-cost sensor. The system based on the FPGA shown in Fig. 8 digitizes the signal from sensor, multiplexes and processes it to obtain four signals and expandible as needed. MATLAB saves, visualizes and analyzes the biosignal. The system is specifically designed to produce a digital output signal that increases over time in accordance with the level of human effort.

The data are incorporated digitally and displayed on MATLAB plotters, as shown in Fig. 19, corresponding to a digital biosignal; this biosignal is presented as an increased voltage in time. Table 5 shows important parameters such as the electrical specifications and basis from processing in the software and hardware.

Table 5.

Proposed system specifications

Parameter	Specifications
RAW Amplitude	100-300 mV
Integrated amplitude	0-4 V
Frequency	50 Hz
Gain	11
CMRR	86-93 dB
ADC Resolution	10-bit
Channels	4
Electrode material	AgCl superficial
Electrode ratio	2.5 cm
Interelectrode distance	5 mm
Processing Hardware	Xilinx Nexys 4 FPGA
Processing software	MATLAB 2024a

In addition to the data, the mathematical calculations required for MU estimation include input data such as the time propagation of the action potential, the action potential amplitude, system information regarding the amplification of the electromyograph, the time constant of the integrator, and the IEMG signal amplitude. All these factors are generated by the instrument designed and generate the final result of the virtual MU data estimation.

The fundamental parameters used [19,20] and instrument specifications were considered important in the experimental protocol and in the final results. It is important to maintain these factors to obtain the same results, and any change in them alters the outcome.

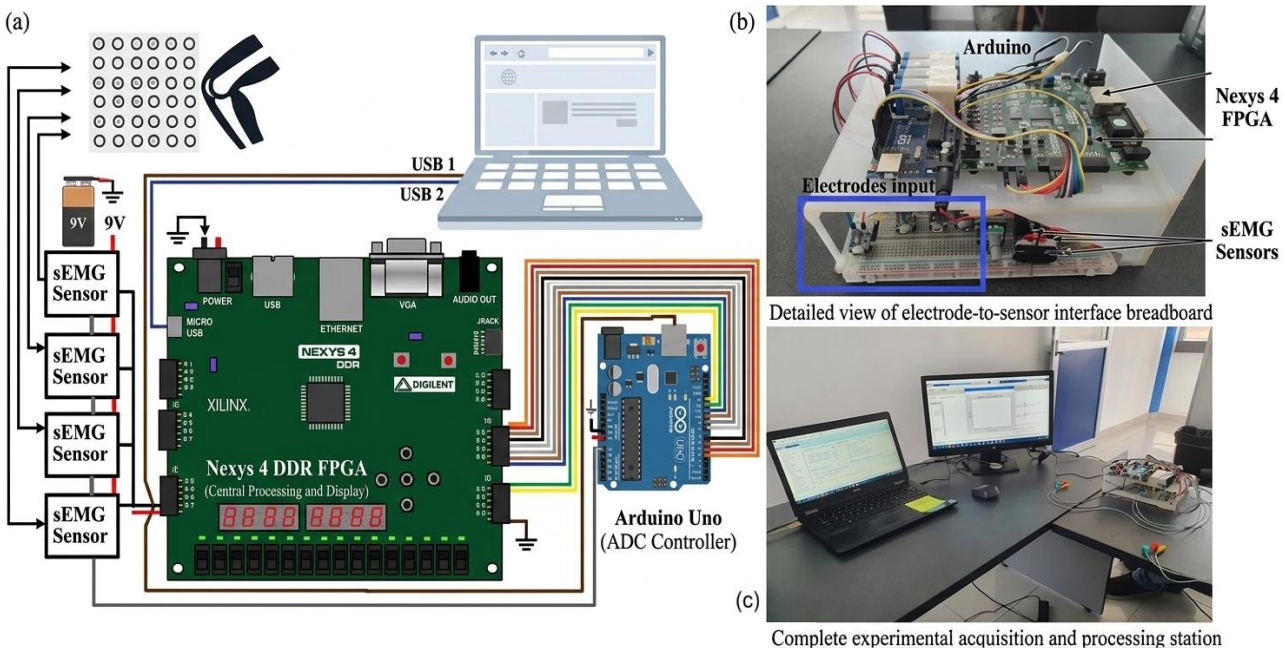


Fig. 19. Four sensors connected to the femoris muscle are used, as shown on the left side of the schematic. Arduino digitalizes the four analog signals. The FPGA processes four analog signals from sensors. MATLAB computer showing the sEMG digital integrated signal: a) virtual instrument, b) physical instrument, and c) experimental station.

5.2 Measurement of sEMG biopotentials

The measurement of the sEMG biopotential routine consists of acquiring electrical signals of the rectus femoris from 7 healthy young persons between 18 and 22 years age to generate a database with information for muscle characterization. The measurement study protocol from the manuscript was reviewed and approved by the Institutional Ethics Committee of the Universidad Politécnica de Guanajuato.

sEMG as shown in Fig. 20 signals were recorded using disposable Ag/AgCl electrodes (45X43 mm adult size). The electrode pairs were positioned differentially over the muscle belly, aligned parallel to the muscle fibers. Due to the physical dimensions of the sensor pads, an edge-to-edge placement was adopted, resulting in a center-to-center inter-electrode distance (IED) of approximately 45mm. While this distance slightly exceeds the conventional SENIAM recommendation, crosstalk was minimized by strictly adhering to anatomical criteria to avoid neighboring muscle boundaries and innervation zones, ensuring a reliable macro-sEMG representation for the force-activation relationship characterization.

The routine begins with four bipolar channels in the matrix positioned in the quadriceps femoris on every person, as shown in Fig. 21 and Fig. 22. They proceeded to extend and flex the knee over a 90 second period, and this procedure was repeated three times in each experiment.

The movement protocol involves the extension and flexion of the left leg of users without load, performing continuous and constant movement between 0 and 90 degrees at the knee joint, as shown in Fig. 10 and 11.

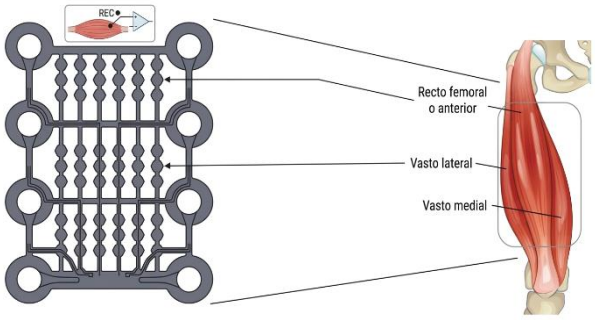


Fig. 20. Electrode matrix mechanical design. Examples of position electrodes in the rectus femoris [32]

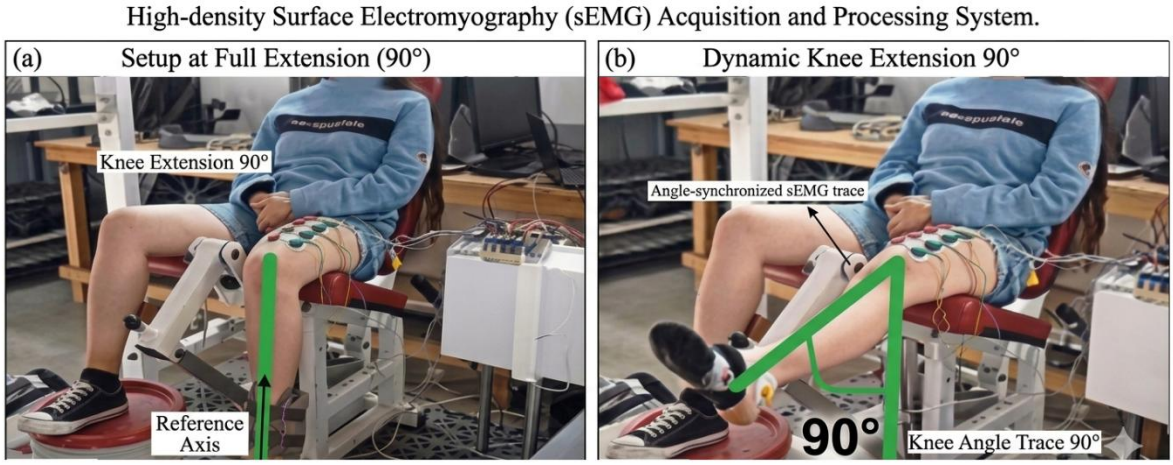


Fig. 21. Movement routine. a) The person was sitting in a chair with knees at 90 degrees to the horizontal. b) Parallel with the horizontal.

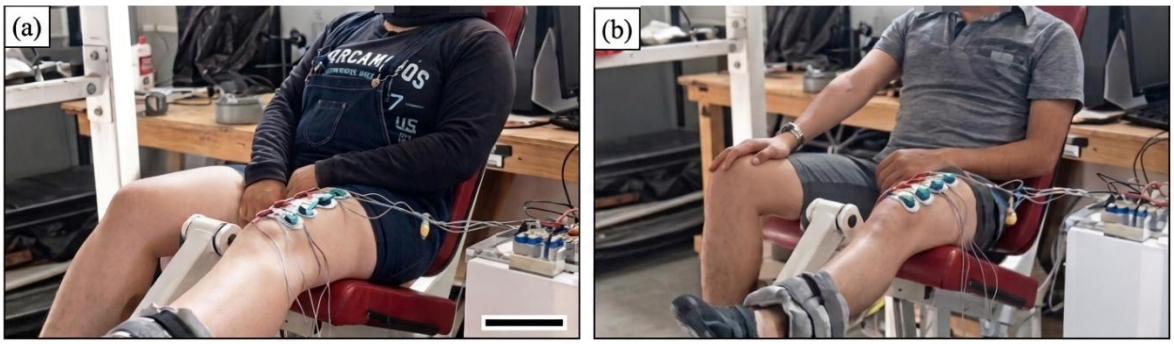


Fig. 22. Movement routine. The person was sitting in a chair with knees in maximum extension. a) Participant 1. b) Participant 2

Declarations

Ethics approval and consent to participate

The measurement study protocol from the manuscript was reviewed and approved by the Institutional Ethics Committee of the Universidad Politécnica de Guanajuato. All procedures performed in this study involving human participants were in strict accordance with the ethical standards of the institutional research committee, the 1964 Declaration of Helsinki and its later amendments. Informed consent was obtained from all individual participants prior to their inclusion in the study.

Consent for publication

Not applicable.

Availability of data and materials

The datasets generated and/or analyzed during the current study are available from the corresponding author on reasonable request.

Competing interests

The authors declare no competing interests.

Funding

This work has been funded by Instituto Politécnico Nacional and Universidad Politécnica de Guanajuato.

Author contributions

YJSF contributed to the conceptualization, methodology, software, investigation, and formal analysis; generated the main idea; designed and developed the instrument and methodology; and analyzed the obtained results.

AHZ supervised and reviewed the research, strengthening the technological development and methodological vision to give greater meaning to the work.

EMS: Provided feedback and redirected the research by contributing new tools for the study and recommending relevant references.

RCL, TSR, and JCPA: Reviewed and provided feedback on the research, meticulously analyzing references and citations, and assisting in the correction of several sections of the manuscript.

Acknowledgements

We are thankful with Instituto Politécnico Nacional, Universidad Politécnica de Guanajuato and SECIHTI.

References

1. Gazzoni M, Barone U. Multi-Channel Surface EMG Detection and Conditioning. Proceedings of the International Congress on Neurotechnology, Electronics and Informatics. 2013;119-25.

2. Kilby J, Prasad K, Mawston G. Multi-Channel Surface Electromyography Electrodes: A Review. IEEE Sensors Journal. 2016;16(14):5510-9.

3. Zhang Y, Chen Y, Yu H, Yang X, Lu W. Learning Effective Spatial–Temporal Features for sEMG Armband-Based Gesture Recognition. IEEE Internet of Things Journal. 2020;7(8):6979-92.

4. Zhu K, Guo W, Yang G, Li Z, Wu H. High-Fidelity Recording of EMG Signals by Multichannel On-Skin Electrode Arrays from Target Muscles for Effective Human–Machine Interfaces. ACS Applied Electronic Materials. 2021;3(3):1350-8.

5. Stachaczyk M, Atashzar S, Farina D. Adaptive Spatial Filtering of High-Density EMG for Reducing the Influence of Noise and Artifacts in Myoelectric Control. IEEE Transactions on Neural Systems and Rehabilitation Engineering. 2020;28(7):1511-7.

6. Zheng M, Crouch MS, Eggleston MS. Surface Electromyography as a Natural Human–Machine Interface: A Review. IEEE Sensors Journal. 2022;22(10):9188-9198.

7. Abu-Faraj ZO, Harris GF, Smith PA, Hassani S. Human Gait and Clinical Movement Analysis. In: Wiley Encyclopedia of Electrical and Electronics Engineering. 2nd ed. New York: John Wiley & Sons, Inc.; 2015. p. 1-34. doi:10.1002/047134608X.W6606.pub2

8. Mendes JJA, Campos DP, de Oliveira RS, de Souza JMS, Pereira LA, de Carvalho ACPLF. AD8232 to Biopotentials Sensors: Open-Source Project and Benchmark. Electronics. 2023;12(4):833. doi:10.3390/electronics12040833

9. Al-Ayyad M, Owida HA, De Fazio R, Al-Naami B, Visconti P. Electromyography Monitoring Systems in Rehabilitation: A Review of Clinical Applications, Wearable Devices and Signal Acquisition Methodologies. Electronics. 2023;12(7):1520. doi:10.3390/electronics12071520

10. De la Peña S, Polo A, Robles-Algarín C. Implementation of a Portable Electromyographic Prototype for the Detection of Muscle Fatigue. Electronics. 2019;8(6):619. doi:10.3390/electronics8060619

11. Rohlen R, Lubel E, Sgambato BG, Antfilk C, Farina D. Spatial Decomposition of Ultrafast Ultrasound Images to Identify Motor Unit Activity – A Comparative Study with Intramuscular and Surface EMG. Journal of Electromyography and Kinesiology. 2023;73:102825. doi:10.1016/j.jelekin.2023.102825

12. Tabasi A, Brouwer NP, Kingma I, van Dijk W, de Looze MP, Moya-Esteban A. The Effect of Back Muscle Fatigue on EMG and Kinematics-Based Estimation of Low-Back Loads and Active Moments During Manual Lifting Tasks. Journal of Electromyography and Kinesiology. 2023;73:102815.

13. Chaparro-Cárdenas SL, Castillo-Castañeda E, Lozano-Guzman AA, Zequera M, Gallegos-Torres RM, Ramirez-Bautista JA. Characterization of Muscle Fatigue in the Lower Limb by sEMG and Angular Position Using the WFD Protocol. Biocybernetics and Biomedical Engineering. 2021;41:933-43. doi:10.1016/j.bbe.2021.06.003

14. Shariatzadeh MJ, Hadizadeh Hafshejani E, Mitchell CJ, Chiao M, Grecov D. Predicting muscle fatigue during dynamic contractions using wavelet analysis of surface electromyography signal. *Biocybernetics and Biomedical Engineering*. 2023;43(2):428–441. doi:10.1016/j.bbe.2023.04.002.

15. Del Vecchio A, Holobar A, Falla D, Felici F, Enoka RM, Farina D. Tutorial: analysis of motor unit discharge characteristics from high-density surface EMG signals. Electromyography and Kinesiology. 2020;53:102426. doi:10.1016/j.jelekin.2020.102426.

16. Sorensen S. Estimating Motor Unit Numbers from a CMAP Scan: Repeatability Study on Three Muscles at 15 Centers. Clinical Neurophysiology Journal. 2023;151:92-9.
17. Kristensen AG. MScanFit Motor Unit Number Estimation and Muscle Velocity Recovery Cycle Recordings in Diabetic Polyneuropathy. Clinical Neurophysiology Journal. 2020;131:2591-9.
18. Schneider C. Motor Unit Number Estimation by MScanFit in Myotonic Dystrophies. Journal of the Neurological Sciences. 2023;451:120728.
19. McManus L, De Vito G, Lowery MM. Analysis and Biophysics of Surface EMG for Physiotherapists and Kinesiologists: Toward a Common Language with Rehabilitation Engineers. Frontiers in Neurology. 2020;11:576729. doi:10.3389/fneur.2020.576729
20. Kountchev R, Mironov R, Nakamatsu K. New Approaches for Multidimensional Signal Processing. In: Proceedings of International Workshop NAMSP 2022, Smart Innovation, Systems and Technologies. Singapore: Springer; 2023. p. 44-55.
21. Genzebu TM. Investigating the Behavior of Charge, Voltage and Current During Charging and Discharging of Capacitor. World Journal of Applied Physics. 2022;7(2):11-20., doi:10.11648/j.wjap.20220702.11.
22. De Carvalho M, Swash M. Muscle Action Potentials: CMAP and motor unit number estimation (MUNE). In: Clinical Neurophysiology. 4th ed. Elsevier; 2014. p. 320-335.
23. Nandedkaar SD, Barkhaus PE, Stalberg E. Motor Unit Number Index: Principle, Method and Findings in Healthy Subjects and in Patients with Motor Neuron Disease. Muscle & Nerve Journal. 2010;42:798-807. doi:10.1002/mus.21824
24. Farina D, Merletti R, Enoka RM. High-density surface EMG: Techniques and applications at a motor unit level. Biocybernetics and Biomedical Engineering. 2012;32(3):3-27. doi:10.1016/S0208-5216(12)70039-6
25. Holobar A, Farina D, Gazzoni M, Merietti R, Zazula D. Estimating Motor Unit Discharge Patterns from High-Density Surface Electromyogram. Clinical Neurophysiology. 2009;120:551-62.
26. Rossi HG, Brussa M, Salvucci F. Development of a Surface Electromyography Module for a Simplified Gait Analysis System. Universidad Nacional de San Martín, Science and Technology. 2019
27. Van Dijk JP, Blok JH, Lapatki BG, van Schaik IN, Zwarts MJ, Stegeman DF. Erratum to: 'Motor unit number estimation using high-density surface electromyography'. Clinical Neurophysiology. 2008;119(10):2383. doi:10.1016/j.clinph.2008.09.001
28. Block JH, Van Dijk JP, Zwarts MJ, Stegeman DF. Motor Unit Action Potential Topography and its Use in Motor Unit Number Estimation. Muscle & Nerve. 2005;32:280-91.
29. Peng Y, He J, Yao B, Li S, Zhou P, Zhang Y. Motor Unit Number Estimation Based on High-Density Surface Electromyography Decomposition. Clinical Neurophysiology. 2016. doi:10.1016/j.clinph.2016.06.014
30. Soto Pérez J, Salazar Lara LV. Ultrasonographic classification of muscle tears. Anales de Radiología en México. 2008;2:121-8.
31. Cieza A, Causey K, Kamenov K, Hanson SW, Chatterji S, Vos T. Global estimates of the need for rehabilitation based on the Global Burden of Disease Study 2019: A systematic analysis for the Global Burden of Disease Study 2019. The Lancet. 2021;396(10267):2006-17. doi:10.1016/S0140-6736(20)32592-7

32. Phairungsakul B. The Effects of a Self-Efficacy Promotion Program and Social Support on Exercise Behavior of Elderly People with Knee Osteoarthritis [thesis]. Chiang Mai: Faculty of Nursing, Chiang Mai Univ.; 2006. p. 1-3.

33. Arnold WD, Sheth KA, Wier CG, Kissel JT, Burghes AH, Kolb SJ. Electrophysiological Motor Unit Number Estimation (MUNE) Measuring Compound Muscle Action Potential (CMAP) in Mouse Hindlimb Muscles. J Vis Exp. 2015;(103):52899. doi:10.3791/52899

34. Chen M, Bashford J, Zhou P. Motor Unit Number Estimation (MUNE) Free of Electrical Stimulation or M Wave Recording: Feasibility and Challenges. Front Aging Neurosis. 2022;14:799676. doi:10.3389/fnagi.2022.799676

35. Jarque-Bou NJ, Sancho-Bru JL, Vergara M. A systematic review of EMG applications for the characterization of forearm and hand muscle activity during activities of daily living: Results, challenges, and open issues. Sensors. 2021;21(9):3035. doi:10.3390/s21093035

36. Chen M, Lu Z, Zong Y, Li X, Zhou P. A novel analysis of compound muscle action potential scan: Staircase function fitting and StairFit motor unit number estimation. IEEE Journal of Biomedical and Health Informatics. 2023;27(3):567-78. doi:10.1109/JBHI.2022.3229211

37. Pavey N, Hannaford A, Higashihara M, van den Bos M, Kiernan MC, Menon P, Vucic S. Utility of split hand index with different motor unit number estimation techniques in ALS. Clinical Neurophysiology. 2023;156:175-82. doi:10.1016/j.clinph.2023.09.018

38. Marsala MJ, Gabriel DA, Inglis JG, Christie AD. How many motor units is enough? An assessment of the influence of the number of motor units on firing rate calculations. Journal of Electromyography and Kinesiology. 2024;75:102872. doi:10.1016/j.jelekin.2024.102872

39. Murillo JL. Electromyography in Rehabilitation Sciences. Rev Mex Investig Cienc Salud. 2021;9(2):45-58. Available from: https://www.redalyc.org/journal/817/81759607022/html/

40. Göker İ. Investigation of the Relationship between the Amplitude of the Maximum Responses of Compound Muscle Action Potential (CMAP) Scan and the Motor Unit Number Estimates (MUNE). 2022 Medical Technologies Congress (TIPTEKNO), Antalya, Turkey; 2022. p. 1-4. doi:10.1109/TIPTEKNO56568.2022.9960149

41. De Carvalho M, Barkhaus PE, Nandedkar SD, Swash M. Motor unit number estimation (MUNE): Where are we now? Clinical Neurophysiology. 2018;129(7):1507-1516.

42. Ali A, Sundaraj K, Ahmad RB, Ahamed NU, Islam A. Surface electromyography for assessing triceps brachii muscle activities: A literature review. Biocybernetics and Biomedical Engineering. 2013;33(4):187–195. doi:10.1016/j.bbe.2013.09.001.

43. Texas Instruments. INA122 Micropower Instrumentation Amplifier [Internet]. Dallas (TX): Texas Instruments; 1997 [actualizado jun 2005; consultado 13 abr 2026]. Disponible en: https://www.ti.com/lit/ds/symlink/ina122.pdf

44. Rojas A, Farfán A, Mora E, Minchala LI, Wong S. Assessing the SNR Influence in the Estimation of the Mean Frequency of Lower Limbs sEMG Signals. IEEE Lat Am Trans. 2018;16(8):2108-2114. doi: 10.1109/TLA.2018.8528223.

45. Yuvaraj M, Raja P, David A, Burdet E, Varadhan SKM, Balasubramanian S. A systematic investigation of detectors for low signal-to-noise ratio EMG signals [version 4; peer review: 2 approved]. F1000Research. 2024;12:429. doi: 10.12688/f1000research.133246.4.

46. Henderson ZJ, Sanzo P, Zerpa C, Kivi D. Ankle bracing's effects on lower extremity iEMG activity, force production, and jump height during a Vertical Jump Test: An exploratory study. Phys Ther Sport. 2019 May;37:171-8. doi: 10.1016/j.ptsp.2019.04.002.

47. Shenoy S, Mishra P, Sandhu JS. Peak torque and iEMG activity of quadriceps femoris muscle at three different knee angles in a collegiate population. J Sports Med Doping Stud. 2011;1(1):102. doi: 10.4172/2161-0673.1000102.

Supplementary Files

This is a list of supplementary files associated with this preprint. Click to download.

- Samanot3.tif
- Samanot4.tif
- Samanot2.tif
- Samanot1.tif
- Samanot5.tif